Enzyme mimicry by the antiidiotypic antibody approach

Alexander V. Kolesnikov*, Arina V. Kozyr*, Elena S. Alexandrova*, Frédéric Koralewski†, Alexander V. Demin‡, Mikhail I. Titov*, Bérangère Avalle†, Alfonso Tramontano§, Sudhir Paul§, Daniel Thomas†, Alexander G. Gabibov*¶, and Alain Friboulet†¶‖

*Shemyakin and Ovchinnikov Institute of Bioorganic Chemistry, Russian Academy of Sciences, 16/10 Mikluho-Maklaya Street, Moscow 117871, Russia; ‡Institute of Gene Biology, Russian Academy of Sciences, 34/5 Vavilov Street, Moscow 117324, Russia; §Center for Chemical Immunology and Therapeutics, Department of Pathology and Lab Medicine, University of Texas, Houston Medical School, 6431 Fannin, Houston, TX 77030; and †Unité 6022 associée Centre National de la Recherche Scientifique, Université de Technologie de Compiègne, BP 20529–60205 Compiègne Cedex, France

Communicated by Jean-Marie P. Lehn, Universite Louis Pasteur, Strasbourg, France, August 1, 2000 (received for review March 7, 2000)

The concept of ''internal image'' of antiidiotypic antibodies has provided the basis for eliciting catalytic antibodies. A monoclonal IgM 9A8 that was obtained as an antiidiotype to AE-2 mAb, a known inhibitor of acetylcholinesterase, displayed esterolytic activity. Study of recombinant Fab fragments and separate light and heavy chains of 9A8 confirmed that the antibody variable domain encodes the catalytic function, whereas neither part of the primary sequence of the Fab exhibited homology with the enzyme. The specific modification of the 9A8 variable domain by an active site-directed covalent inhibitor revealed the presence of an active site Ser residue. A three-dimensional modeling suggests the existence of a functional catalytic dyad Ser-His. Comparison of active sites of 9A8 and 17E8 esterolytic abzyme raised against transition-state analog revealed structural similarity although both antibodies were elicited by two different approaches.

Apart from its natural function, the humoral immune response represents an *in vivo* system capable of generating a molecular imprint of virtually any natural or synthetic compound. In recent years, the unique ability of antibodies to evolve rapidly toward maximum complementarity to the input substance was exploited successfully for eliciting antibodies with tailored catalytic activities. Most of these catalysts (abzymes) were created by immunization with template molecules, designated as transition-state analogs (TSAs), which are stable mimics of rate-limiting transient states or intermediates of the chemical transformation (1–3).

As proposed by Niels Jerne (4), and later supported by experimental data (5), antiidiotypic antibodies can recognize antigenic determinants that overlap a portion of the Ab1-combining site that contacts the original antigen. Hence, the combining site of the antiidiotypic antibody may carry an ''internal image'' of this antigen. This idea, in turn, has led to the hypothesis that antigenic mimicry properties of antiidiotypic antibodies could be used to elicit antibodies with the functional features of enzyme active sites.

In particular, structural and functional mimicry of an enzyme active site by autoantibodies emerging from disregulation of the idiotypic network was suggested to explain spontaneous occurrence of abzymes in autoimmune disease (6–8). The proposal is supported further by the successful application in obtaining antibodies with cholinesterase-like (9) and β-lactamase activities (10). Specifically, mice immunized with a monoclonal IgG, AE-2, that displayed both high specificity to the active site of human erythrocyte acetylcholinesterase (AcChoE) and strong inhibition of the enzyme activity produced a monoclonal IgM (antiidiotype) with activity similar to that of the parental enzyme (9).

Materials and Methods

Catalytic AE-2 and Immunological Properties of 9A8. Mouse monoclonal IgG AE2 directed against the active site of human erythrocyte AcChoE was purified from mice ascites fluid on an Affi-Gel protein A column (Bio-Rad) as detailed by the manufacturer's instructions. Monoclonal IgM 9A8 was purified from mice ascites fluid by fractionation on FPLC gel filtration on a Sephacryl S-200 h 10/50 column (Pharmacia) in 0.1 M phosphate buffer, pH 7.4, followed by ion-exchange chromatography on ceramic hydroxyapatite (Bio-Rad). The latter column was run with a gradient of phosphate buffer increasing from 10 to 400 mM and pH increasing from 6.8 to 8.

The BIAcore analysis was done by using sensor chips precoated with streptavidin. Each binding/elution cycle was performed with a constant flow of PBS (5 μl/min). A 30-μl aliquot of anti-mouse IgG Fc-specific biotinylated conjugate (100 μg/ml) was injected, followed by the addition of 30 μl of AE-2 (900 μg/ml).

AcChoE activity of 9A8 was measured in solution by Ellman's method (11). Various concentrations of acetylthiocholine iodide were added in the presence of 1.6 mM 5,5′-dithiobis(2-nitrobenzoic acid) (DTNB), and the substrate hydrolysis was followed at 405 nm.

Cloning, Sequencing, and Expression of 9A8 Fab Fragment. Total RNA from hybridoma 9A8 was isolated, and cDNA was synthesized as described (12). First-strand synthesis was performed with primers 1 and 2. Primer 1 was based on the C-terminal sequence of the light chain, including the Cys residue. Primer 2 corresponds to residues 218–223C of the μ heavy chain. The light chain gene was amplified by PCR with primers 1 and 3 and then with primers 21 + 23 and 22 + 23 to append 5′-*Fse*I and 3′-*Asc*I sites, respectively. Amplification product was inserted into *Fse*I and *Asc*I sites to vector pEF2. Primer 3 structure was deduced as the result of N-terminal sequencing of the light chain, which yielded the sequence DVVMTQ. Because N terminus of the heavy chain was blocked (most likely as the pyroglutamate), 16 independent PCRs were performed for the heavy chain amplification with primer 2 and 16 degenerative primers 5–20 encompassing most of known leader sequences of mouse heavy chains. PCR was performed with Pfu polymerase (Stratagene) by using standard procedures. Amplification yielded products from primers 7, 8, 12, and 19. Sequencing of amplification products obtained from these different primers revealed identity of amplified heavy chains. Heavy chain N terminus primer 4 was derived from these sequence data. A V_H + C_{H1} gene was

Abbreviations: TSA, transition-state analog; AcChoE, acetylcholinesterase; BtChoEase, butyrylcholinesterase; CDR, complementarity determining regions; VH, VL, the variable domains of the heavy (H) and light (L) chains; DTNB, 5,5′-dithiobis(2-nitrobenzoic acid).

Data deposition: The sequences reported in this paper have been deposited in the GenBank database (accession nos. AF253060 and AF253061).

¶A.G.G. and A.F. contributed equally to this work.

‖To whom reprint requests should be addressed. E-mail: Alain.Friboulet@utc.fr.

The publication costs of this article were defrayed in part by page charge payment. This article must therefore be hereby marked "*advertisement*" in accordance with 18 U.S.C. §1734 solely to indicate this fact.

Article published online before print: *Proc. Natl. Acad. Sci. USA*, 10.1073/pnas.200360497. Article and publication date are at www.pnas.org/cgi/doi/10.1073/pnas.200360497

amplified with primers 2 and 4, then with 24 + 25 to introduce 5′-*Sfi*I and 3′-*Not*I, and the product was inserted between the cognate sites of pEF2. Sequences of the primers used in this work are as follows: (1) 5′-ACACTCATTCCTGTTGAAG-3′; (2) 5′-TGGAATGGGCACATGCAGATCTCT-3′; (3) 5′-GATGTTGTGATGACCCAA[C,T]T-3′; (4) 5′-CAGGTCCAGCTGCAGCAGTCT-3′; (5) 5′-CC[A,C,G]TTCC[G,T]GGTATCCTGTC-3′; (6) 5′-T[T,C][G,C]CAAGCTGTGTCCT[A,G,T]TC-3′; (7) 5′-[G,T]CA[A,G][T,G]A[T,A]CTGCAGGT[G,T]TCC-3′; (8) 5′-CAACAGC[T,C]ACAGGTGTCCA-3′; (9) 5′-GTGGTTACAGGGGTCAATT-3′; (10) 5′-TTA[C,A]ATGGTATCCAGTGT; (11) 5′-T[T,A]TTAAAA[G,A]G[G,T]GTCCAG[T,A]GT-3′; (12) 5′-ACTGCAGGTGTCCACTCT-3′; (13) 5′-TTCTTCCTGTCAGTAACT-3′; (14) 5′-ATGGCAGCTGCCCAAAGT-3′; (15) 5′-CCTTCCGGGTATCCTGTC-3′; (16) 5′-[C,T]TTTAAATGGTATCCAGT-3′; (17) 5′-[G,A]CAACT[G,A]CAGGTGTCC[A,T]CT-3′; (18) 5′-ACATTCCCAAGCTGT[G,A]TCCT-3′; (19) 5′-GCAACAGCTACAGGTGTCC-3′; (20) 5′-CTTATATTATGGACTGTTTGT-3′; (21) 5′-CAGCCGGCGATGGCCGATGTTGTGATGACCCAA-3′; (22) 5′-ACTACTCTAAGGCCGGCCTGCTGCTCCTCGCTGCCCAGCCGGCGATGGCC-3′; (23) 5′-TATTACTTATGGCGCGCCGCTAACACTCATTCCTGTTGAAG-3′; (24) 5′-TATATCAATTTGGCCCAGCCGGCCATGGCCCAGGTCCAGCTGCAGCAGTCT-3′; and (25) 5′-ATTCTTATAAGCGGCCGCTGGAATGGGCACATGCAGATCTCT-3′.

The plasmid pEF2 is a dicistronic vector based on pET22b(+) (Novagen). The vector allows independent cloning, expression, detection, and purification of both separate antibody chains and Fab fragment. Cloning of the antibody chain genes is performed into two pairs of octanucleotide-cutting endonucleases: *Sfi*I and *Not*I for heavy chain V_H-C_{H1} fragment and *Fse*I and *Asc*I for the complete light chain. Insertion of *Sfi*I into the leader peptide has been described previously (13). *Fse*I was inserted into the pelB sequence during vector construction by silent mutagenesis. This way of insertion allows correct cleavage of cloned chains by leader peptidase, yielding native termini of the expression products targeted to the periplasm. Sequences encoding a c-myc peptide and His_6 tag are inserted downstream to the heavy chain constant region to facilitate detection and purification procedures. An additional c-myc tag is placed downstream to the light chain gene for detection of the light chain in the absence of the heavy chain. However, in the Fab construct, its translation is blocked by PCR-based addition of the UAG stop codon.

Plasmid pEF2 with assembled antibody chain genes was used for electroporation of BL21(DE3) cells. The periplasmic fraction was loaded on an IDA-Sepharose column charged with 0.2 M Co^{2+}, and the expressed protein was eluted by linear pH gradient by using solutions A and B (50 mM NaH_2PO_4/100 mM NaCl, pH 4.0). A final purification was done by affinity chromatography on immobilized anti-c-myc antibodies.

Catalytic and Immunological Properties of Expressed Fragments. Recognition of idiotypic antibody AE-2 by recombinant fragments was measured by ELISA. Assays were done in standard 96-well plates (Costar) according to the following protocol. Samples were dispensed at 2.5 μg/ml (Fab fragments, light and heavy chains) in 50 mM carbonate buffer, pH 9.6, 100 μl/well, and were incubated for 1 h at 37°C. The plate then was blocked by adding 1% gelatin in PBS and washed three times with PBS/0.1% Tween 20. The wash step was repeated after each subsequent incubation step. AE-2 (120 nM) was added and incubated in PBS/0.1% Tween 20 for 1 h at 37°C. Bound AE-2 was revealed by adding goat anti-mouse Fc-specific biotinylated conjugate (Sigma) diluted 1:4,000 in PBS/0.1% Tween 20 in each well for 30 min at 37°C. Incubation with 1:2,500 Vectastain avidin-peroxidase in PBS for 30 min at room temperature was followed by development with a 0.3 mg/ml 2,2′-azinobis(3-ethylbenzthiazoline-sulfonic acid) and 0.05% H_2O_2 solution in 25 mM citrate buffer, pH 5. Measurement of the optical density at 410 nm was recorded after a 15- and 30-min incubation at room temperature.

AcChoE activity of different expressed fragments was measured by Ellman's method as described above.

Identification of Catalytic Residues and Modeling of the 9A8 Active Site. For denaturation, reduction, and S-alkylation, 50 μg of the protein was dissolved in 200 μl of 0.1 M NH_4HCO_3. A freshly prepared solution of DTT was added to a final concentration of 5 mM, and the mixture incubated at 50°C for 20 min. After cooling to room temperature, iodoacetamide was added to 25 mM and the mixture was kept in the dark at room temperature for 30 min.

To prepare a tryptic protein digest for MS peptide mapping, protein samples were reduced and alkylated as described above. Sequencing-grade trypsin (Roche, Gipf-Oberfrick, Switzerland) was added to yield a final enzyme-to-substrate ratio of 1:20 (wt/wt), and the mixture was incubated at 37°C for 4 h. The reaction was quenched by 5% trifluoroacetic acid, bringing the pH of the mixture to below pH 4.0

The computer program GPMAW (General Peptide Mass Analysis for Windows) was used for computer-assisted proteolytic peptide mapping (14, 15).

Molecular Modeling. A model was constructed with the Swiss Model program by using a homologous antibody of known structure for the input coordinates (16, 17). Verification of the model, performed by using the Biotech Validation Suite for Protein Structures (European Molecular Biology Laboratory), revealed that 98.9% of the amino acids of the model fell in the allowed regions of the Ramachandran plot. The structure of 9A8 was fitted to that of 17E8 by superposition of their Cα atoms using program O (Silicon Graphics, Mountain View, CA) and SWISS PDB VIEWER (Microsoft Windows).

Results and Discussion

Catalytic and Immunological Properties of 9A8. Catalytic mAb 9A8, raised according to the antiidiotypic concept of structural and functional mimicry, was found to emulate AcChoE activity. Esters were hydrolyzed with efficiency ($k_{cat}/K_M = 1.35 \times 10^5$ M^{-1} sec^{-1} for acetylthiocholine) higher than those observed in the case of esterolytic abzymes raised via the TSA approach (2, 3). To avoid possible contamination of mAb preparations by enzymes, efficient protocols for purification of the IgM abzyme were developed. It also has been shown that the parental AE-2 mAb inhibits the catalytic activity of 9A8 (9). To determine binding parameters of the idiotypic/antiidiotypic mAb pair, we studied interaction of AE-2 with 9A8 by surface plasmon resonance (18) (Fig. 1). Formation of the idiotype/antiidiotype complex rapidly reached equilibrium. A ratio of k_{on}/k_{off} of 2.26×10^9 M^{-1} for the complexation reaction reflected a value characteristic of high-affinity antibodies.

We have demonstrated previously that the hydrolytic activity of 9A8 is characterized by a relaxation of specificity toward both substrates and inhibitors as compared with AcChoE (9). A specific feature of serine esterases, and of AcChoE in particular, is the specific irreversible inhibition by organophosphorous compounds (19). To further characterize the hydrolytic mechanism, we used the phosphonylating agents depicted below (20) (Schemes 1 and 2).

The release of a fluorogenic (I) or chromogenic (II) product in the chemical reaction with nucleophilic residues also is convenient for titration of the enzyme active site.

Although compounds I and II were shown to be efficient active-site phosphonylating agents of butyrylcholinesterase (BtChoEase), they failed to inhibit human AcChoE (Fig. 2*A*). However, incubation of compound I with monoclonal IgM 9A8 was accompanied by loss of esterase activity of the abzyme. This modification yielded a detectable increase in fluorescence resulting from release

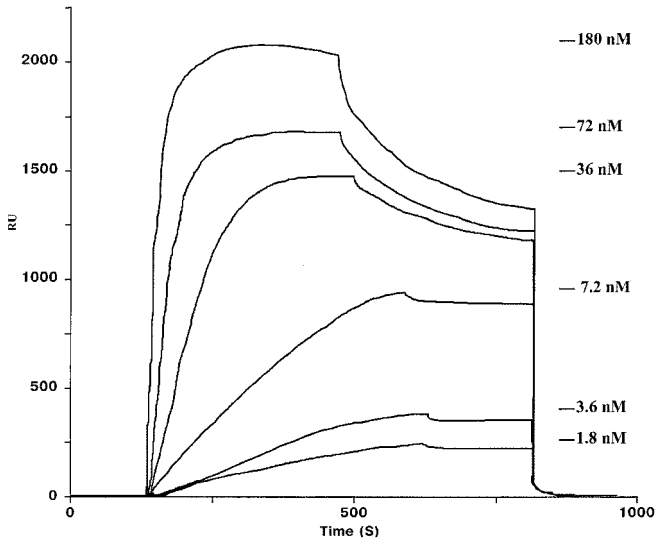

Fig. 1. BIAcore analysis of affinity binding between idiotype AE2 and antiidiotype 9A8. Binding of different concentrations of 9A8 to immobilized AE-2 is presented on the sensorgrams. The binding constant was calculated from the experimental curve by nonlinear regression analysis (k_{on}/k_{off} = 2.26 10^9 M^{-1}).

of the coumarin group. The reaction with compound II was shown to result in the specific modification of the catalytic antibody heavy chain, as detected by avidin-peroxidase staining of electroblotted proteins (Fig. 2*B*). The minimal concentration of compound II required for staining is in good accord with the concentrations of biotinylated phosphonates used for specific labeling of esterases and proteases (21, 22), thus strongly supporting a mechanism-based process for biotinylation of 9A8 by II.

The pseudo-first-order rate constant for modification by I of BtChoEase and 9A8 was found to be $k_1$mod = 0.062 min^{-1} and

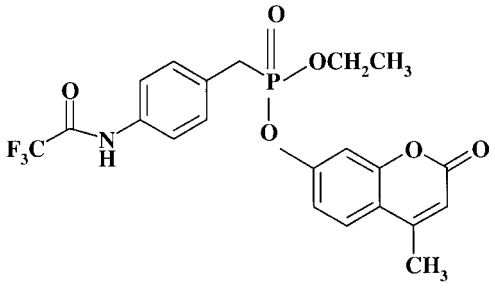

Scheme 1. Compound I: Coumarinyl ethyl *p*-trifluoroacetamidophenyl methylphosphonate.

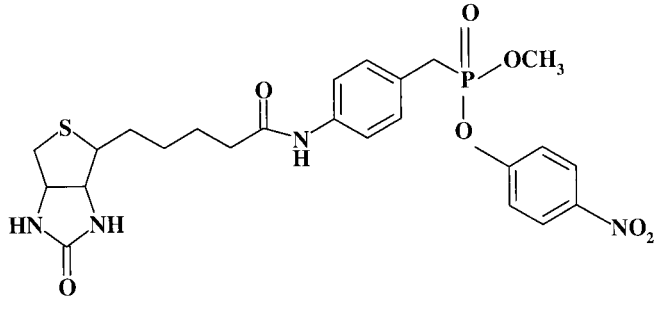

Scheme 2. Compound II: Nitrophenyl methyl *p*-biotinamidophenylmethylphosphonate.

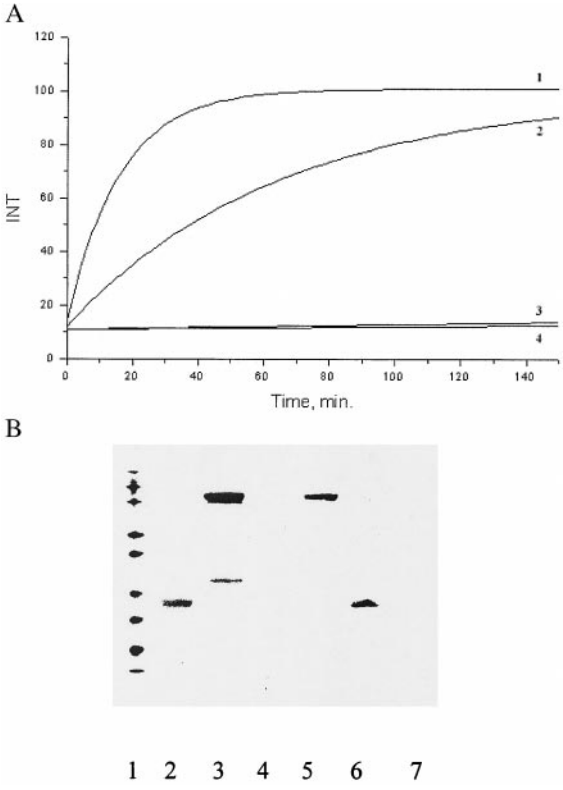

Fig. 2. Modifications of cholinesterase enzymes and antiidiotypic mAb by MCA-phosphonate. (*A*) Kinetics of interaction of MCA-phosphonate (compound I) with BtChoEase (**1**) and AcChoE (**3**) enzymes and with 9A8 (**2**) and IgM 2H11 (**4**) antibodies. Assays were performed on an Aminco spectrofluorimeter (excitation, 365 nm, and emission, 450 nm). Protein concentration was 55 nM, and substrate concentration was 1 μM in PBS, pH 7.8. (*B*) Modification of 9A8 mAb H chain by compound II. Protein concentration was 5.5 pM, and substrate concentration was 100 pM in PBS, pH 7.8. Western blot shown was stained by neutravidin-HRP conjugate. Lanes: 1, 10-kDa molecular mass markers; 2, trypsin modified by biotinylated 4-(2-aminoethyl)-benzenesulfonyl fluoride (AEBSF); 3, 9A8 modified by biotinylated AEBSF; 4, monoclonal IgM 2H11 modified by biotinylated AEBSF; 5, 9A8 modified by compound II; 6, trypsin modified by compound II; 7, monoclonal IgM 2H11 modified by compound II.

0.0154 min^{-1}, respectively. These data suggest kinetically equivalent reactivity of active-site nucleophiles in the two biocatalysts.

Lack of AcChoE modification by I is not surprising considering the three-dimensional structure of the enzyme active center (23, 24). This indicates that the catalytically active serine residue is buried in a very narrow cavity.

On the contrary, the butyrylcholinesterase structure shows that the active center is closer to the surface and therefore accessible to reaction with a larger hydrophobic substrate (24). Thus, the ability of the antiidiotypic mAb to react with compound I suggests that the potential active center of the abzyme adopts a more relaxed conformation compared with AcChoE.

Cloning, Sequencing, and Expression of 9A8 Fab Fragment. Heavy (H) and light (L) chain cDNAs encompassing the Fab fragment of the 9A8 antiidiotypic mAb were cloned and sequenced (GenBank accession nos. AF253060 and AF253061). Analysis of light and heavy chain variable regions (Fig. 3*A*) did not show any significant homology with the primary structure of AcChoE. Thus, the antiidiotypic abzyme active center bears no direct resemblance to its enzyme progenitor at the primary structure level.

To permit expression of the abzyme as a Fab fragment in *E. coli*, we designed a dicistronic vector suited for functional

A

Light chain

gat gtt gtg atg acc caa act cca ctc tcc ctg cct gtc agt ctt gga gat caa gcc tcc atc tct tgc aga tct agt cag agc
D V V M T Q T P L S L P V S L G D Q A S I S C R S S Q S
_____CDR1_____
att gta cac agt aat aga tac acc tat tta gat tgg tac ctg cag aaa cca ggc cag tcg cta aag ctc ctg ata tat ggg gtt
I V H S N R Y T Y L D W Y L Q K P G Q S L K L L I Y G V
_CDR2_____
tcc aac cga ttt tct ggg gtc cca gac agg ttc agt ggc agt gga tca ggg aca gat ttc aca ctc aag atc agc aga gtg
S N R F S G V P D R F S G S G S G T D F T L K I S R V
_____CDR3_____
gag gct gag gat atg gga gtt tat tac tgc ttt caa ggt aca cat gtt ccg tac acg ttc gga ggg ggg acc aag ctg gaa
E A E D M G V Y Y C F Q G T H V P Y T F G G G T K L E

ata aaa cgg
I K R

Heavy chain

cag gtc cag ctg cag cag tct ggg gct gaa ctg gca aaa cct ggg gcc tca gtg aag ctg tcc tgc aag gct tct ggc tac
Q V Q L Q Q S G A E L A K P G A S V K L S C K A S G Y
____CDR1_____
aac ttt act agc tac tgg atg cac tgg gta aaa cag agg cct gga cag ggt ctg gaa tgg att gga tac att aat cct agc
T F T S Y W M H W V K Q R P G Q G L E W I G Y I N P S
_____CDR2_____
agt ggt tat act aag tac aat cag aag ttc aag gac aag gcc aca ttg act gca gac aaa tcc tcc agc aca gcc tac atg
S G Y T K Y N Q K F K D K A T L T A D K S S S T A Y M
_____CDR3_____
cag ctg agc agc ctg aca tat gag gac tct gca atc tat tac tgt gca aga tcg tac tac ggt cct gac tac tgg ggc caa
Q L S S L T Y E D S A V Y Y C A R S Y Y G P D Y W G Q

ggc acc act ctc aca gtc tcc tca
G T T L T V S S

B

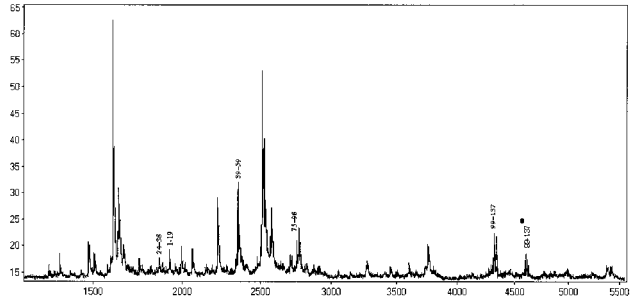

Fig. 3. (*A*) Primary structure of variable regions of antiidiotypic mAb 9A8. *S*, active-site Ser (CDR 3 of H chain); *H*, active-site His (CDR 1 of H chain). (*B*) Matrix-assisted laser desorption ionization–time-of-flight mass spectrum of a tryptic digest of reduced and S-alkylated antiidiotypic mAb 9A8. About 5 pmol peptide mixture was used in the dried-droplet method of sample preparation, with 2,5-dihydroxybenzoic acid as a matrix. The spectrum was recorded in reflectron positive-ion mode on Vision 2000 (ThermoBioanalysis, Waltham, MA). Tryptic peptides of H chain variable region found are assigned. ●, Peptide with a Ser modified by compound I.

assembly of the Fab in *E. coli* periplasmic space. In the Fab construct the sequence encoding L chain contained no additional downstream coding regions, whereas the H chain fragment was ligated in-frame with a C-terminally positioned c-myc peptide and His_6 tag, thus allowing efficient detection and purification of the expressed Fab and separate $V_{H1}C_{H1}$. Western blot analysis of *E. coli* periplasmic extracts obtained after induction of expression with isopropyl β-D-thiogalactoside indicated the presence of two bands of 28 and 50 kDa that were characteristic of the H chain fragment and the corresponding Fab, respectively. Treatment of periplasmic extracts with 10 mM DTT before electrophoresis and blotting eliminated the upper band, supporting its assignment as the Fab. Expression of separate L chain and $V_{H1}C_{H1}$ fragment was done in the same vector, modified to produce only one of polypeptides, each fused to C-terminal c-myc and His_6 tags. Both constructs yielded 28-kDa periplasmic polypeptides as judged by Western blotting (Fig. 4).

After successful production of 9A8 Fab, it was necessary to investigate whether it retained a functional combining site and catalytic activity. Interaction of various recombinant 9A8 fragments with AE-2 mAb was studied by ELISA. To do this, we analyzed binding of AE-2 to separately expressed L chain, $V_{H1}C_{H1}$ fragment, or Fab fragment coated on microtiter plates. AE-2 appeared to have no affinity for the L chain, whereas it clearly displayed binding to the recombinant Fab and, to a lesser extent, to the $V_{H1}C_{H1}$ polypeptide alone. Analysis of purified recombinant antibody fragments revealed that the integrity of the antibody-combining site is indispensable for expression of the abzyme function. The Fab fragment assembled in *E. coli* periplasm exhibited significant catalytic activity, whereas neither $V_{H1}C_{H1}$ nor L chain alone was active. Moreover, hydrolysis of acetylthiocholine depended on the 9A8 Fab concentration and was inhibited by the addition of the idiotypic mAb AE-2 to the reaction. Apart from the abzyme inhibition, AE-2 exhibited reduced, yet significant affinity to the separate H chain, thus providing indirect evidence for location of the principal elements responsible for the transfer of the enzyme image within this subunit.

Identification of Catalytic Residues and Modeling of the 9A8 Active Site. Previously reported chemical modification of monoclonal IgM 9A8 by the organophosphorous compound echothiopate and by diethyl pyrocarbonate was indicative of the involvement of both serine and histidine residues in the hydrolytic mechanism (9). Experiments described above with compounds I and II further supported the crucial role of a serine or other nucleophilic residue in catalysis mediated by the antiidiotypic abzyme.

To identify the active-site catalytic group, we analyzed tryptic digests of the Fab prepared from the 9A8 IgM, both before and after reaction with phosphonate ester I, using the matrix-assisted laser desorption ionization–time-of-flight mass spectrometry technique. Analysis of the digested, unmodified Fab revealed complete agreement in the structure of peptides with the fragments deduced from the cDNA sequences, thus confirming identity of the cloned sequences to those of the original 9A8.

Furthermore, comparison of the mass spectrum of 9A8 Fab digest modified by phosphonate I with that of the unmodified Fab digest revealed a shift of the peak corresponding to peptide 99–137 of the H chain (Fig. 3*B*). This peptide includes the entire complementarity determining region H3 (CDRH3) and 32 downstream amino acid residues. The calculated difference in the mass of the two peaks, Δ MW = 293 mass units, was in agreement with the mass of the phosphonylating compound I after displacement of the coumarinyl group. There are eight serine residues present within the sequence of peptide 99–137 of the H chain, and, therefore, additional studies are necessary to identify which of these is involved in the catalytic mechanism. At the same time, several lines of evidence suggest SerH99 to be the functional nucleophile. Polyclonal mouse IgM as well as monoclonal IgM 2H11 specific to H^+Na^+ATPase gave no detectable reaction with compound II, thus indicating that CDRH3 or adjacent downstream sequences in the irrelevant IgM did not provide reactive groups capable of nonspecific phosphonylation. The presence of a catalytic His-Ser dyad in the antiidiotypic abzyme active site is suggested both by the observed pattern of the catalyst inhibition and by the proposed molecular mimicry of the cholinesterase mechanism (19). This, in turn, implies juxtaposition of the Ser to a His residue to permit the hydrogen bond formation. Only three His residues were found in the 9A8 Fab, making it feasible to deduce the most likely dyad structure from a three-dimensional molecular model of 9A8 Fab fragment.

A first approximation model was constructed with the SWISS MODEL program, using a homologous antibody of known structure for the input coordinates (16, 17). Computer analysis revealed that His35 from CDR1 of the H chain is located and oriented at the appropriate distance for hydrogen bonding interaction with the side chain hydroxyl of Ser99, a likely nucleophilic residue within the modified tryptic peptide 99–137. No Asp, Glu, or additional His residues were found correctly positioned in the model to be involved in a possible catalytic triad

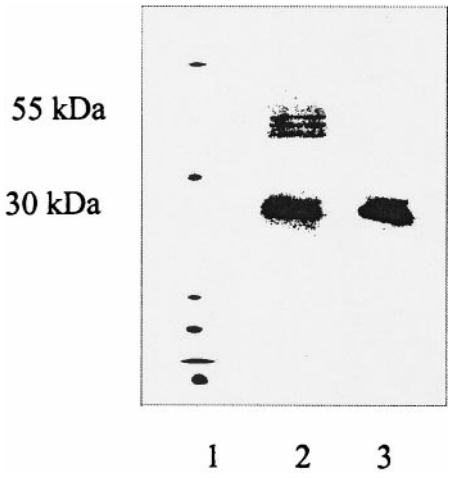

Fig. 4. Assembly of recombinant of 9A8 Fab fragment in *E. coli* periplasm. Western blot stained by anti-c-myc antibody. Lanes: 1, molecular mass markers; 2, without mercaptoethanol; 3, incubation with mercaptoethanol.

(Fig. 5). As revealed by the model, the putative dyad is located in the middle of the shallow cleft between H and L chain CDR loops. Considering the above-described structural differences of AcChoE and BtChoEase, a partial explanation for the relaxed specificity of the catalytic antibody in comparison with the parental enzyme can be rationalized.

Previous studies suggested that certain antibodies can develop a serine protease-like activity by entirely natural means, unrelated to experimental immunization with antienzyme antibodies or TSAs (25, 26). The catalytic Ser and His residues in such antibodies appear to be located in the L chain subunit. In contrast, the residues responsible for catalysis in the present study were found in the H chain, consistent with the conclusion that the catalytic activity of our mAb is derived by experimentally induced enzyme mimicry, as opposed to a fortuitous immunological event. Heavy chain His35 was found to be a principal catalytic residue in several antibody esterases raised by the TSA approach, as it is likely to be the case in our antibody. It was shown to participate both in general base and in covalent catalysis (27–31). In addition, HisH35 is implicated in the stabilization of negative charge in the transition state of esterolysis catalyzed by the 43C9 abzyme and is essential for catalytic activity of this antibody (32–34). Importantly, mAb 43C9 provides an example of catalysis through a covalent acyl-abzyme intermediate, with another histidine, HisL91, participating as the principal nucleophile. Notably, active sites of esterolytic anti-TSA antibodies CNJ206, 48G7, 43C9, and 17E8, described to possess an active His35 residue, appeared to be structurally convergent (35).

Sequence comparison revealed significant homology of 9A8 V_H to the corresponding domains of the His35 convergent family. Analysis of L chains indicated that V_L domains 9A8 and 43C9 bear more similarity to each other than to the sequences of the other family members. Furthermore, V_H domains of 9A8 and 17E8 abzymes share 80% sequence homology, which is much higher than the 48% identity shared by 17E8 and its close structural analog, CNJ206. Strikingly, as in the case of 9A8, the 17E8 abzyme also contained SerH99, which potentially completes a catalytic dyad. Based on this observation, we compared the available crystal structure of 17E8 Fab (30, 31) with the 9A8 3-D model.

Although 17E8 CDRH3 is 3 aa longer than 9A8 CDRH3, superposition of the structures (Fig. 5) reveals significant similarity between their proposed active centers, thus outlining the

Table 1. Catalytic properties of esterolytic antibodies 9A8 and 17E8 and their recombinant Fabs

Catalyst	k_{cat}, sec^{-1}	K_M, mM	$k_{cat}/K_m \times 10^3$ $M^{-1}\cdot s^{-1}$	Ref.
9A8	81	0.6	135	9
Recombinant 9A8 Fab	2.8	16.6	0.16	
17E8	3.71	0.45	8.24	31
17E8 Fab	0.85	0.26	3.27	31
Recombinant hu17E8 Fab	0.98	0.58	1.69	38

Catalytic parameters of 9A8 and recombinant Fab fragment of 9A8 were determined by using acetylthiocholine as substrate. Catalytic parameters of 17E8, 17E8 Fab, and recombinant humanized 17E8 Fab (hu17E8) were obtained by using L-phenyl ester of *N*-formylnorleucine as described in refs. 31 and 38.

phenomenon of structure–function convergence of catalytic antibodies elicited via completely different methodologies. Convergent evolution of the anti-TSA esterolytic antibodies was attributed mainly to the structural similarity of TSAs used to elicit these abzymes, whereas limitations of the immune response are thought to play a secondary role (29, 35). On the contrary, 9A8 abzyme was raised as an esterase antiidiotype, thus extending the phenomenon of structure–function convergence beyond the family of anti-TSA catalysts. Comparison between catalytic properties of 17E8 and 9A8 abzymes and their Fabs is shown in Table 1. A significant decrease in catalytic activity observed in the recombinant 9A8 Fab can be attributable to the presence of improperly folded species and folding intermediates in the Fab preparation (36, 37).

The fidelity of transfer of the enzyme active center image by the idiotypic network approach is, at present, unclear. Numerous studies have shown that antiidiotypic mAbs can attain functional activity similar to that of the original antigen (5). The relevant crystallographic data indicate that in some cases CDRs of the antiidiotypic antibodies may mimic fragments of the primary structure of the antigen, whereas in other cases they emulate only a three-dimensional or topological structural feature. We have found no similarity of linear amino acid sequences between mammalian AcChoE and 9A8. At the same time, labeling of the

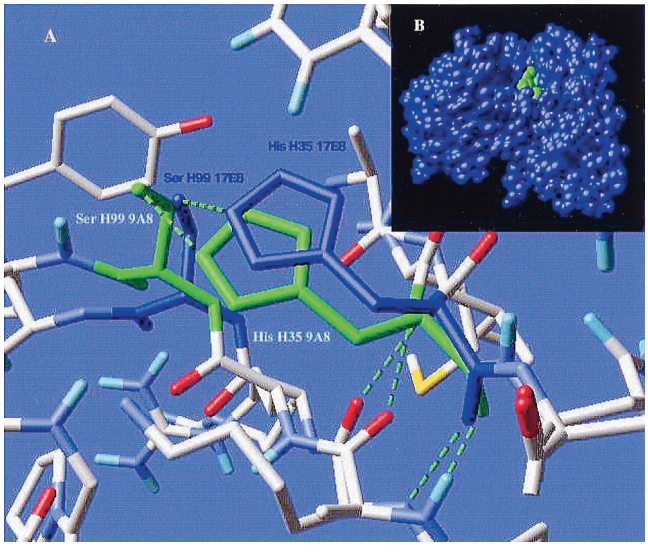

Fig. 5. Rendered images of 9A8-combining site. (*A*) The similarity of His H35–Ser H99 dyad of 9A8 esterolytic antibody (green) and His H35–Ser H99 dyad of 17E8 esterolytic antibody (blue) is illustrated. (*B*) Rendered image of broad combining site cavity. Catalytic HisH35–Ser H99 dyad of 9A8 is colored green.

active-site nucleophile and computer modeling of the 9A8 Fab suggests involvement of the Ser-His dyad in the catalytic process. Thus, the mode of action of the 9A8 mAb resembles a cholinesterase with relaxed specificity and with high kinetic efficiency when compared with other esterolytic antibodies. This notion is supported by the data on the steady-state kinetic constants determined for hydrolysis of the generic esterase substrate *p*-nitrophenyl acetate by 9A8 mAb: $k_{cat} = 37\ sec^{-1}$ and $K_M = 0.34$ mM.

Conclusions

Molecular analysis of 9A8 abzyme yielded important information about the expression of catalytic activity via the idiotypic network. That both AcChoE and 9A8 possess high affinity to the idiotypic mAb AE-2 leads to the assumption that the enzyme active site and the antiidiotypic mAb-combining site share at least some structurally similar epitopes. Because no linear sequence similarity was found between these two entities, we are led to conclude that the mimicry phenomenon is mainly of a topological nature. However, this idiotypic image transfer phenomenon is able to preserve the expression of catalytic residues in a correct position and orientation necessary for a functional hydrolytic machinery. Prokaryotic expression of recombinant 9A8 Fab fragment reveals that the complete Fab assembling is required for catalytic activity as well as for interaction with the idiotypic mAb AE-2, thus implicating complex conformational entities involving the H and L chains for specific binding and catalysis. Similarity of the proposed active centers of 9A8 and 17E8 esterolytic mAbs is particularly interesting considering that, to the best of our knowledge, even among anti-TSA abzymes there is no other example of putative catalytic Ser-His dyads found both at the primary and at the three-dimensional structural level.

Inhibition of catalytic activity of mAb 9A8 by diethyl pyrocarbonate (9) and by organophosphorous compounds, along with the mass spectral data, indicates that 9A8 provides a nucleophile for catalysis and suggests the involvement of the His-Ser dyad in the mechanism of ester hydrolysis. At the same time, compelling evidence on the covalent catalytic mechanism of 17E8 remains to be obtained (38, 39). Covalent catalysis proceeding through an acyl-abzyme intermediate is a feature of another mAb containing HisH35 in the active center, 43C9 (32–34). Unlike 9A8, comparative mass spectral analysis of mutants and natural 43C9 species showed that the principal nucleophilic residue is HisL91. This difference validates the alternative mode of mass spectral study used in the case of 9A8, because mutations at HisH35 likely would have failed to identify the nucleophilic group among catalytic residues of the antiidiotypic abzyme. Structural convergence observed among catalytic antibodies elicited among phosphonate TSAs raised the concern about limited capacity of the immune system to produce catalysts with efficiencies approaching that of enzymes. At present, it is not possible to determine whether the similarity observed between 9A8 and anti-TSA abzymes emerged as a random event or whether it reflects a reproducible pattern of the esterolytic immune response. The latter may be a sign of significant constraints imposed by the immune system on the expression of structural determinants for catalytic activity. On the other hand, analysis of the structural convergence phenomenon could provide abzyme templates that could be evolved into efficient catalysts by using methods for antibody selection based on catalytic activity instead of binding capacity.

Our results demonstrate that the idiotypic network is able to elicit catalytic antibodies that carry the functional imprint of enzymatic active sites. In the case of 9A8 mAb, not only is the esterolytic activity emulated, but general mechanistic features and principal catalytic determinants are likely to be recapitulated. At the same time, the second-sphere residues of the active-center layout differ significantly between the antiidiotype and its prototype AcChoE, thus pointing to the different solutions used by enzymes and abzymes in the evolution of mechanistically similar catalytic activity. Reproduction of the serine hydrolase catalytic machinery in 9A8 abzyme holds the promise that the idiotypic network is capable of functional emulation of even more sophisticated active centers such as those of serine amidases and proteases.

This work was supported in part by grants from the European Union INCO-COPERNICUS program (IC15 CT96-0909), International Association for Cooperation with scientists from the former Soviet Union (96-1386), the Russian Fund for Fundamental Research, the Scientific Schools Program, and the Russian Program for Advanced Protein Engineering.

1. Jencks, W. P. (1969) in *Catalysis in Chemistry and Enzymology* (McGraw–Hill, New York), p. 288.
2. Tramontano, A., Janda, K. D. & Lerner, R. A. (1986) *Science* **234,** 1566–1570.
3. Pollack, S. J., Jacobs, J. W. & Schultz, P. G. (1986) *Science* **234,** 1570–1573.
4. Jerne, N. K. (1974) *Ann. Immunol.* **125C,** 373–389.
5. Pan, Y., Yuhasz, S. C. & Amzel, L. M. (1995) *FASEB J.* **9,** 43–49.
6. Bronshtein, I. B., Shuster, A. M., Shechenko, L. V., Gromova, I. I., Kvashuk, O. A., Geva, O. M. & Gabibov, A. G. (1995) *Mol. Biol. (Russia)* **23,** 1553–1557.
7. Bronshtein, I. B., Shuster, A. M., Gololobov, G. V., Gromova, I. I., Kvashuk, O. A., Belostotskaya, K. M., Alekberova, Z. S., Prokaeva, T. B. & Gabibov, A. G. (1992) *FEBS Lett.* **314,** 259–263.
8. Shuster, A. M., Gololobov, G. V., Kvashuk, O. A., Bogomolova, A. E., Smimov, I. V. & Gabibov, A. G. (1992) *Science* **256,** 665–667.
9. Izadyar, L., Friboulet, A., Remy, M. H., Roseto, A. & Thomas, D. (1993) *Proc. Natl. Acad. Sci. USA* **90,** 8876–8880.
10. Avalle, B., Thomas, D. & Friboulet, A. (1998) *FASEB J.* **12,** 1055–1060.
11. Ellman, G. L., Courtney, K. D., Andres, V. & Featherstone, R. M. (1964) *Biochem. Pharmacol.* **7,** 88–95.
12. Sambrook, J., Fritsch, E. F. & Maniatis, T. (1989) *Molecular Cloning: A Laboratory Manual* (Cold Spring Harbor Lab. Press, Plainview, NY).
13. Winter, G., Griffiths, A., Hawkins, R. E. & Hoogenboom, H. E. (1994) *Annu. Rev. Immunol.* **12,** 433–455.
14. Laessing, U., Giordano, S., Stecher, B., Lottspeich, F. & Sturmer, C. A. O. (1994) *Differentiation* **56,** 21–29.
15. Kussmann, M., Lassing, U., Sturmer, C. A. O., Przybylsky, M. & Roepstorff, P. (1997) *J. Mass Spectrom.* **32,** 483–493.
16. Peitsch, M. C., Welles, T. N., Stampf, D. R. & Sussman, J. L. (1995) *Trends Biochem. Sci.* **20,** 82–84.
17. Guex, N. & Peitsch, M. C. (1997) *Electrophoresis* **18,** 2714–2723.
18. Brigham-Burke, M., Edwards, J. R. & O'Shannessy, D. J. (1992) *Anal. Biochem.* **205,** 125–131.
19. Quinn, D. M. (1987) *Chem. Rev.* **87,** 955–979.
20. Tramontano, A., Ivanov, B., Gololobov, G. V. & Paul, S. (2000) *Appl. Biochem. Biotechnol.* **83,** 233–243.
21. Abuelvaman, A. S., Jackson, D. S., Hudig, D., Woodard, S. L. & Power, J. C. (1997) *Arch. Biochem. Biophys.* **344,** 271–280.
22. Glynn, P., Read, D. J., Guo, R., Wylie, S. & Johnson, M. K. (1994) *Biochem. J.* **301,** 551–556.
23. Soreq, H., Gnatt, A., Loewenstein, Y. & Neville, L. F. (1992) *Trends Biochem. Sci.* **17,** 353–358.
24. Radic, Z., Pickering, N. A., Vellom, D. C., Camp, S. & Taylor, P. (1993) *Biochemistry* **32,** 12074–12084.
25. Paul, S., Mei, S., Mody, B., Eklund, S. H., Beach, C. M., Massey, R. J. & Hamel, F. (1991) *J. Biol. Chem.* **266,** 16128–16134.
26. Gao, Q. S., Sun, M., Rees, A. & Paul, S. (1995) *J. Mol. Biol.* **253,** 658–664.
27. Patten, P. A., Gray, N. S., Yang, P. L., Wedemayer, G. J., Boniface, J. J., Stevens, R. C. & Schultz, P. G. (1996) *Science* **271,** 1086–1091.
28. Charbonnier, J. B., Carpenter, E., Gigant, B., Golinelli-Pimpaneau, B., Eshhar, Z., Green, B. S. & Knossow, M. (1995) *Proc. Natl. Acad. Sci. USA* **92,** 11721–11725.
29. Charbonnier, J. B., Golinelli-Pimpaneau, B., Gigant, B., Tawfik, D. S., Chap, R., Schlinder, D. S., Kim, S. H., Green, B. S., Eshhar, Z. & Knossow, M. (1997) *Science* **275,** 1140–1142.
30. Zhou, W., Guo, J., Huang, W., Fletterick, R. J. & Scanlan, T. S. (1994) *Science* **265,** 1059–1064.
31. Guo, J., Huang, W. & Scanlan, T. S. (1994) *J. Am. Chem. Soc.* **116,** 6062–6069.
32. Stewart, J. D., Krebs, J. F., Siuzdak, G., Berdis, A. J., Smithrud, D. B. & Benkovic, S. J. (1994) *Proc. Natl. Acad. Sci. USA* **91,** 7404–7409.
33. Krebs, J. F., Siuzdak, G., Dyson, H. J., Stewart, J. D. & Benkovic, S. J. (1995) *Biochemistry* **34,** 720–723.
34. Thayer, M. M., Olender, E. H., Arvai, A. S., Koike, C. B., Canestrelli, I. L., Stewart, J. D., Benkovic, J. D., Getzoff, E. D. & Roberts, V. A. (1999) *J. Mol. Biol.* **291,** 329–345.
35. McBeath, G. & Hilvert, D. (1996) *Chem. Biol.* **3,** 433–445.
36. Skerra, A. & Plückthun, A. (1991) *Protein Eng.* **4,** 971–979.
37. Humphreys, D. P., Weir, N., Lawson, A., Mountain, A. & Lund, P. A. (1996) *FEBS Lett.* **380,** 194–197.
38. Baca, M., Scanlan, T. S., Stephenson, R. C. & Wells, J. A. (1997) *Proc. Natl. Acad. Sci. USA* **94,** 10063–10068.
39. Arkin, M. R. & Wells, J. A (1998) *J. Mol. Biol.* **284,** 1083–1094.